

# **MULTI-SCALE INDENTATION AND SCRATCH BEHAVIOR OF OXIDE GLASSES**

**KASIMUTHUMANIYAN S**



**DEPARTMENT OF MATERIALS SCIENCE AND ENGINEERING  
INDIAN INSTITUTE OF TECHNOLOGY DELHI**

**JULY 2023**

**© Indian Institute of Technology Delhi (IITD), New Delhi, 2023**

**MULTI-SCALE INDENTATION AND SCRATCH  
BEHAVIOR OF OXIDE GLASSES**

by

**Kasimuthumanian S**

Department of Materials Science and Engineering

Submitted in fulfilment of requirements of degree of  
Doctor of Philosophy

to the



**INDIAN INSTITUTE OF TECHNOLOGY DELHI**

**JULY 2023**

# Declaration

I hereby declare that the thesis contains the work carried out in fulfillment of the requirements for the award of the degree of Doctor of Philosophy under the guidance and supervision of **Prof. Nitya Nand Gosvami**, Associate Professor, Department of Materials Science and Engineering and **Prof. N. M. Anoop Krishnan**, Associate Professor, Department of Civil Engineering, IIT Delhi. The contents of the dissertation, including text, tables, figures, etc., have not been reproduced from other reports, theses, etc. Wherever reproduction has been made from books, journals, reports, manuals, websites, etc., the sources have been duly acknowledged and referenced appropriately.

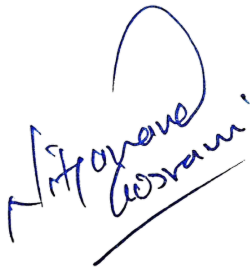


Kasimuthumaniyan S

July 2023

# Certificate

This is to certify that the thesis entitled *Multi-scale Indentation and Scratch Behavior of Oxide Glasses* is being submitted by **Mr. Kasimuthamaniyan S** to the Indian Institute of Technology Delhi for the award of the degree of **Doctor of Philosophy**. This is a record of the research work and is entirely carried out by him under my supervision and guidance. The research report presented in this thesis has not been submitted for the award of any other degree or diploma.



**Prof. Nitya Nand Gosvami**

Associate Professor

Department of Materials Science and Engineering  
Indian Institute of Technology Delhi



**Prof. N. M. Anoop Krishnan**

Associate Professor

Department of Civil Engineering  
Indian Institute of Technology Delhi

# Acknowledgements

The circumstances under which I have started writing this thesis were really challenging for me. So, first and foremost, I would like to express my profound and sincere gratitude to my supervisors, **Prof. Nitya Nand Gosvami** and **Prof. N. M. Anoop Krishnan** for their excellent guidance, encouragement and motivation which helped me to complete this thesis. This thesis would not have been possible without their timely and untiring guidance and support. They have given me excellent freedom to carry out the research plans in the manner I wished to execute. They constantly motivated me whenever I was down with failed experiments. Their valuable input and ideas while performing my experiments has greatly helped in completing the experiments successfully.

I would also like to thank SRC members Prof. Rajesh Prasad, Prof. Jayant Jain, and Prof. Shashank Bishnoi for providing me with invaluable feedbacks, constructive criticisms and serving on my committee during the tenure. Those comments had helped to improve my thesis work. I would also like to thank Dr. Allu Amarnath Reddy, CSIR-CGCRI, Kolkata, for helping with the aluminophosphosilicate and sodium borate glass samples. I would also like to extend my thanks to Prof. Morten Smedskjaer, Aalborg University, Denmark, for the borosilicate glass samples. I want to thank the Department of Materials Science and Engineering for allowing me to use various instruments and taking care of my official needs. Special mention to Mr. Mohit, Mr. Brijesh, and Mr. S. B. Prasad for allowing me to access and learn various scientific pieces of equipment here at IIT Delhi.

The road to research is an arduous one and the only thing that makes it pleasant is the camaraderie with the lab fraternity. Special thanks to Sourav Sahoo for helping me in my data analysis and sharing his late-night research thoughts without expecting anything back in return. I would like to thank my friend Dr. Shrikanth for giving thoughtful suggestions while writing my thesis. Special thanks to my beloved colleagues – Dr. Deepak Kumar Chauhan, Dr.

Himanshu Vashishtha, Dr. Vickey Nandal, Dr. Amit Prasad, Dr. Prashant Mittal, Dr. Gaurav, Dr. Shanta, Dr. Aditya Gokhale, Dr. Nooruddin Ansari, Dr. Aravi Muzaffar, Dr. Ranjeet Kumar, Dr. Chetan Singh, Mr. Abhishek Rastogi and Mr. Himanshu Rai for making the workspace a lively place to work and learn. I would also like to extend my thanks to NTM3 and M3RG lab colleagues – Dr. Ravinder, Dr. Rajesh, Dr. Amreen, Ms. Shweta Rani Keshri, Mr. Suresh Bishnoi, Mr. Mohd Zaki, Mrs. Tanu Pittie, Mr. Ashish Yadav. Thanks to Mr. Deepak Choubey, Lab Manager, M3RG lab, for organizing all the lab apparatus and equipment required for my work. Special thanks to Mr. Indrajeet Mandal for lending his helping hand in sample preparation. Though his entry in my research journey was towards the end, I wish I could have got such helping colleague at very early stage of my research. I would also like to extend my thanks to my other colleagues for their critical help towards the end of my research project – Mr. Subhakar Mangam, Mr. Syed Junaid, Mr. Sajid Mannan, Shaikh Junaid.

Most importantly, I am extremely glad to acknowledge my family's unconditional love and encouragement in this research journey. Nothing can ever compensate the time lost in being away from them during my research. My parents, Mr. K. Subramanian and Mrs. Revathi, and sister Sowmiya; my niece Jonisha kutty, my whole sisters' family, my uncle Chandrabose & family. No words cannot describe this feeling of pride.

I want to thank my supervisors **Dr. N. M. Anoop Krishnan** and **Dr. Nitya Nand Gosvami** again for accepting me as I am. I would like to acknowledge them for really uplifting my spirits despite my failures.

Specially, I would like to dedicate this thesis to my dad and mom for their upbringing and the countless sacrifices, support, and trust they gave me to become the person I am today.

**KASIMUTHUMANIYAN S (Suresh)**

# Abstract

Owing to their optical transparency and chemical stability, oxide glasses are used in a range of applications varying from interactive displays, laboratory glasswares to nuclear waste immobilization. Determination of mechanical properties is critical for application of glasses for abovementioned applications. Indentation technique is a popular choice to measure the mechanical response of such oxide glasses due to the convenience in sample preparation and reliable data acquisition from small specimen volume. Various mechanical properties of oxide glasses to mention a few such as hardness, elastic modulus, crack resistance, scratch resistance can be measured by employing indentation technique. The central aim of this thesis is to explore the use indentation technique in studying the mechanical response of various oxide glasses.

Hardness is one of the important properties of glasses which is measured from their indentation response. However, hardness depends strongly on the method of measurement. Initially, we estimate the hardness of three oxide glasses, namely, pure silica (0B), borosilicate (37B), and sodium borate (75B) glass samples at micro and nanoscale. Mechanical polishing is usually carried out to prepare the glass surface required for such indentation tests and can result in generation of residual stress that can change near-surface glass properties significantly. It was observed in this study that annealing of these glass samples, after polishing, has little effect on their hardness and modulus. Interestingly, it was noticed that the nanoindentation is unable to capture the full extent of elastic recovery, thereby underestimating the hardness of these glasses. Such post-indentation elastic recovery is highly dependent on the chemical composition of glass. Combining nanoindentation and atomic force microscopy (AFM) imaging, the complete elastic recovery of glass samples was accurately captured, thereby calculating the true hardness values from indentation depth profiles. Pile-ups surrounding the

residual imprint are also considered in the true hardness estimation. Overall, it is shown that post-indentation elastic recovery plays a crucial role in determining the hardness of glasses.

Further, to investigate the composition-dependent indentation deformation response of glasses, range of borosilicate glasses having varying network formers (Si/B) ratio with constant network modifiers was employed. The borosilicate glasses were annealed below their corresponding glass transition temperature following the nanoindentation measurements to evaluate the extent of densification and shear flow as a function of its composition. Intriguingly, we noticed that the volume recovery upon annealing is inversely proportional to the hardness of the glasses. This implies that the resistance to permanent deformation is closely related to the network connectivity of the glasses, which in turn controls the mechanism of deformation under sharp contact loading. The significant role of alkali and alkaline earth modifiers in modulating the composition-dependent indentation behavior of the borosilicate glass series is shown.

Despite having attractive features, the inherent brittle nature of oxide glasses limits their use in load-bearing and structural applications. Hence, reducing the brittleness behavior of oxide glasses is necessary to improve its reliability and service life for potential applications. With this objective, in this thesis, we also report on the mechanical behavior of the ion-exchanged sodium alumino-phosphosilicate based oxide glasses as a function of chemical strengthening duration. Interestingly, a massive improvement in the crack resistance of oxide glass was observed with respect to the ion-exchange duration. The glasses were able to sustain loads as high as 150 N without the initiation of strength reducing radial cracks on the surface which is almost 1400% increase from the base glass crack resistance value of 11.2 N. This was achievable within 30 minutes of ion-exchange duration. Also, elasto-plastic behavior with regards to normal and lateral loading is also studied to explore the glass' use for scratch applications. Further, the scratch damage resistance was also improved due to ion-exchange

strengthening. Overall, this thesis discusses the composition-dependent indentation deformation of oxide glasses, duration-dependent indentation, and scratch behavior of ion-exchanged oxide glasses.

## सार

अपनी ऑप्टिकल पारदर्शिता और रासायनिक स्थिरता के कारण, ऑक्साइड ग्लास कई अनुप्रयोगों में प्रयोग किए जाते हैं, जैसे कि इंटरैक्टिव डिस्प्ले, प्रयोगशाला ग्लासवेयर और न्यूक्लियर अपशिष्ट स्थायन। उपरोक्त अनुप्रयोगों के लिए ग्लास का यांत्रिक गुणसूत्रण निर्धारित करना महत्वपूर्ण है। इंडेंटेशन तकनीक छोटे सैंपल आयाम से नमूना तैयारी और विश्वसनीय डेटा प्राप्ति के लिए सुगमता के कारण ऑक्साइड ग्लास के यांत्रिक प्रतिक्रिया का मापन करने के लिए एक लोकप्रिय विकल्प है। इंडेंटेशन तकनीक का उपयोग करके कुछ ऑक्साइड ग्लास के विभिन्न यांत्रिक गुणसूत्र, जैसे कि हार्डनेस, प्रतिस्थान अभिवृद्धि, टूटने की प्रतिरोध, खरोंच प्रतिरोध आदि, मापे जा सकते हैं। इस थीसिस का मुख्य उद्देश्य विभिन्न ऑक्साइड ग्लास के यांत्रिक प्रतिक्रिया का अध्ययन करने में इंडेंटेशन तकनीक का उपयोग करना है।

हार्डनेस ग्लास की महत्वपूर्ण गुणों में से एक है, जिसका मापन उनकी इंडेंटेशन प्रतिक्रिया से किया जाता है। हालांकि, हार्डनेस मापने का तरीका परमाणु प्रमाण पर पूरी तरह से निर्भर करता है। पहले, हमने तीन ऑक्साइड ग्लास, जैसे कि प्योर सिलिका (0B), बोरोसिलिकेट (37B) और सोडियम बोरेट (75B) ग्लास के हार्डनेस का अनुमान लगाया, जिसे माइक्रो और नैनोस्केल पर किया गया। मैकेनिकल पॉलिशिंग आम तौर पर उन ग्लास सतह को तैयार करने के लिए किया जाता है, जिसके परिणामस्वरूप शेष तनाव का उत्पन्न होना संभव है जो नजदीकी सतह वाले ग्लास गुणों को बदल सकता है। इस अध्ययन में देखा गया कि इस प्रकार के ग्लास के पॉलिशिंग के बाद इन ग्लास सैंपल्स को बुलाया गया है, उनकी हार्डनेस और मॉड्यूलस पर कोई भी प्रभाव नहीं होता है। रुचिकर है कि नैनोइंडेंटेशन इलास्टिक पुनर्प्राप्ति को पूरी तरह

से पकड़ नहीं पाता है, इससे इन ग्लासेज की हार्डनेस को अग्रहीत किया जाता है। इस प्रकार की पोस्ट-इंडेंटेशन इलास्टिक पुनर्प्राप्ति ग्लास के रासायनिक संरचना पर अधिक निर्भर करती है। नैनोइंडेंटेशन और ऐटमिक फोर्स माइक्रोस्कोपी (AFM) इमेजिंग को मिलाकर, ग्लास सैंपल्स की पूर्ण इलास्टिक पुनर्प्राप्ति को सटीक रूप से पकड़ा गया, इससे इंडेंटेशन गहराई प्रोफाइल से सही हार्डनेस मूल्यों की गणना की गई। शेष निर्माण परिप्रेक्ष्य में भी पूर्ण हार्डनेस अनमूलन का ध्यान दिया गया। समग्र रूप से यह दिखाया गया है कि इंडेंटेशन के बाद की इलास्टिक पुनर्प्राप्ति ग्लास की हार्डनेस निर्धारण में महत्वपूर्ण भूमिका निभाती है।

आगे बढ़कर, ग्लास के संबंधितता के आधार पर इंडेंटेशन रूपांतरण प्रतिक्रिया की अध्ययन-उपयोगी जाँच के लिए, स्थिर नेटवर्क संशोधकों के साथ भिन्नता वाले बोरोसिलिकेट ग्लास की विभिन्न रेंज का प्रयोग किया गया। नैनोइंडेंटेशन परिमाण के बाद इन बोरोसिलिकेट ग्लास को उनके संबंधित ग्लास ओवरगैजन तापमान से नीचे अभिषेक किया गया था जिससे इसके संशोधन के रूप में विधि के साथ दंसन और शियर प्रवाह की मात्रा का मूल्यांकन किया जा सके। रुचिकर है कि हमने देखा कि उन ग्लासेज के बारे में उनके ओवरगैजन के अभिषेक के पश्चात खुलने वाले आयाम के बिल्कुल विपरीत अवरोध होता है। यह इस बात का संदर्भ करता है कि उन ग्लासों के नेटवर्क संबंधितता से हमेशा के लिए विरोध होता है, जिससे यह निर्धारित होता है कि नेटवर्क संबंधितता उन ग्लासों के यांत्रिक प्रतिक्रिया के संचालन पद्धति को नुकसान या टांग बाधने वाले लोडिंग के तहत परिवर्तन करती है। बोरोसिलिकेट ग्लास श्रृंखला के संबंधितता पर अल्काली और अल्कलाइन अर्थ संशोधकों की महत्वपूर्ण भूमिका का प्रदर्शन किया गया है।

ऑक्साइड ग्लास की स्वाभाविक खुरदरापनीयता के बावजूद, उनकी आकर्षक विशेषताएं उन्हें लोड उठाने और संरचनात्मक अनुप्रयोगों में प्रयोग की सीमित करती हैं। इसलिए, ऑक्साइड ग्लास की खुरदरापनीयता व्यवहार को कम करना उनके विश्वसनीयता और संभावित अनुप्रयोगों में सेवाएं के लिए आवश्यक है। इस उद्देश्य से, इस थीसिस में, योजना रूपांतरण समय के संबंध में आयन विनिमयित सोडियम एल्युमिनो-फॉस्फोसिलिकेट आधारित ऑक्साइड ग्लास के यांत्रिक व्यवहार पर भी रिपोर्ट किया गया है। दिलचस्पी से, ऑक्साइड ग्लास की टूटने की प्रतिरोध क्षमता में सोडियम एल्युमिनो-फॉस्फोसिलिकेट ग्लास के यांत्रिक व्यवहार के संबंध में एक महान बदलाव देखा गया। इस समय से सम्बंधित एक्सचेंज के भीतर, ग्लास सतह पर शक्ति के बढ़ते हुए आधारित रेडियल टूटने के आरंभ के बिना, उन्हें 150 N तक लोडों का सहारा देने में सक्षम थे, जो बेस ग्लास टूटने की प्रतिरोध के मूल्य 11.2 N से लगभग 1400% तक वृद्धि है। यह 30 मिनट योजना रूपांतरण के भीतर संभव हो गया था। इसके अलावा, उन्हें समरूपी और अनुकूली भार पर विकसित करने के लिए इलास्टो-प्लास्टिक व्यवहार भी अध्ययन किया गया है जिससे की ग्लास का उपयोग खरोंच प्रतियोगिताओं के लिए किया जा सके। इसके अतिरिक्त, आयन विनिमयन की मजबूती के कारण, खरोंच क्षति प्रतिरोध भी सुधार दिया गया। समग्र रूप से, इस थीसिस में ऑक्साइड ग्लास की संरचना-विशेषित इंडेंटेशन विकृति, समय-विशेषित इंडेंटेशन और आयन विनिमयित ऑक्साइड ग्लास के खरोंच व्यवहार का चर्चा किया गया है।

# Table of Contents

Certificate.....	i
Acknowledgements.....	ii
Abstract.....	iv
List of Figures.....	xiii
List of Tables.....	xvii
Chapter 1 - Introduction.....	1
1.1 Introduction.....	1
1.2 Types of Glasses.....	1
1.3 Mechanical Response of Oxide Glasses.....	3
1.4 Organization of the Thesis.....	5
Chapter 2 - Literature Review.....	6
2.1 Introduction.....	6
2.2 Mechanical Behavior of Glasses.....	6
2.2.1 Why Indentation Tests for Studying the Mechanical Behavior of Glasses?.....	6
2.3 Fundamentals of Indentation.....	8
2.3.1 Densification and Shear Flow.....	11
2.3.2 Indentation Cracking.....	12
2.3.3 Chemical Composition Dependent Indentation Behavior of Oxide Glasses.....	14
2.3.4 Fracture toughness ( $K_c$ ) measurements from indentation.....	15
2.3.5 Loading rate effect on the mechanical behavior of glasses.....	16
2.4 Indentation vs Scratching.....	18
2.5 Scratch Test of Oxide Glasses.....	20
2.6 Scratch Resistance/Scratch Hardness Models.....	21
2.8 Scratch damage evolution in oxide glasses.....	25
2.9 Scratch Induced Deformation Study in Oxide Glasses.....	28
2.10 Effect of Polishing.....	30
2.11 Borosilicate Glasses.....	30
2.12 Ion-exchange Strengthening.....	32
2.13 Summary and Conclusions.....	34
Chapter 3 - Motivation and Objectives.....	35
3.1 Motivation.....	35
3.2 Objectives.....	37
Chapter 4 - Experimental Methodology.....	38

4.1 Introduction .....	38
4.2 Glass Preparation.....	38
4.3 Sample Preparation .....	39
4.4 Material Characterization Techniques .....	40
4.4.1 Differential Scanning Calorimetry .....	40
4.4.2 Indentation Techniques.....	41
4.4.3 Microscopy Techniques.....	47
4.5 Summary .....	49
Chapter 5 - Understanding the Role of Post-indentation Recovery, Pile-up, and Surface Condition on the Hardness of Oxide Glasses .....	50
5.1 Introduction .....	50
5.2 Materials and Methods .....	51
5.2.1 Glass Preparation.....	51
5.2.2 Sample Preparation.....	52
5.2.3 Indentation Experiments.....	53
5.2.4 Elastic-Reconstruction Approach.....	53
5.3 Micro-scale Indentation of Glasses .....	56
5.4 Nanoscale Indentation of Glasses .....	57
5.5 AFM Study of Residual Indents.....	61
5.6 Analysis of the Indentation Depth Profile.....	63
5.7 Conclusions .....	69
Chapter 6 - Indentation Deformation Study of Borosilicate Glasses.....	71
6.1 Introduction .....	71
6.2 Materials and Methods .....	72
6.2.1 Glass Preparation.....	72
6.2.2 Sample Preparation.....	74
6.2.3 Nanoindentation Experiments .....	74
6.2.4 Indentation Deformation Analysis.....	74
6.2.5 Densification Estimation .....	75
6.2.6 Shear flow estimation .....	77
6.3 Nanoindentation of Borosilicate Glasses .....	78
6.3.1 Analysis of Load-displacement Curve .....	78
6.3.2 Elasto-plastic Analysis .....	79
6.4 Effect of Composition on Microhardness and Nanohardness.....	83
6.4.1 Microhardness and Nanohardness .....	83

6.4.2 Role of <i>R</i> and <i>K</i> Ratios on Hardness .....	84
6.5 Indentation deformation mechanisms .....	86
6.5.1 Indentation Pile-up Estimation .....	86
6.5.2 Estimation of volume recovery.....	88
6.5.3 Estimation of Volume Pile-up .....	91
6.5.4 Linking Hardness and Volume Recovery.....	92
6.6 Conclusions .....	94
Chapter 7 - Indentation and Scratch Behavior of Ion-exchanged Sodium Aluminophosphosilicate Glass.....	95
7.1 Introduction .....	95
7.2 Materials and Methods .....	96
7.2.1 Glass Preparation.....	96
7.2.2 Sample Preparation.....	96
7.3 Nanoindentation Experiment.....	98
7.3.1 QCSM Analysis.....	98
7.3.2 Load-Displacement Curve Analysis.....	99
7.3.3 Scratch Hardness Measurements .....	101
7.3.4 Elasto-Plastic Analysis under Normal and Lateral Contacts.....	103
7.4 Crack Resistance Measurements .....	105
7.5 Scratch Damage Evolution.....	108
7.6 Conclusions .....	109
Chapter 8 - Conclusions and Future Work .....	110
8.1 Conclusions .....	110
8.2 Future Work .....	111
8.2.1 Corrosion Study of Borosilicate Series .....	111
8.2.2 Scratch Study of Borosilicate Series .....	112
8.2.3 Multi-pass Scratch Study using Tribometer .....	112
8.2.4 Nano-wear Study .....	112
References.....	114
Appendices.....	138
Publications and Conferences .....	145
CURRICULUM VITAE.....	148

# List of Figures

		<b>Page No.</b>
Figure 2.1	Schematic representation of indentation tests	7
Figure 2.2	(a) Typical Force-displacement curve obtained using nanoindentation (b) Residual imprint indicating the contact depth ( $h_c$ ) at maximum force ( $F_{max}$ ), and final residual depth ( $h_f$ ) after the removal of indenter ( <i>Dey &amp; Mukhopadhyay, 2014</i> ).	9
Figure 2.3	Schematic diagram of indentation deformation stages ( <i>Rouxel et al., 2010</i> )	10
Figure 2.4	Scanning electron micrograph of alkali silicate glass using sharp indenter tip ( <i>K. W. Peter, 1970</i> )	11
Figure 2.5	Optical micrographs of different oxide glass systems taken using Vickers indenter tip (a) – (f): At room temperature, indentation load of 9.81 N with a dwell time of 15 s was recorded. $\nu$ values from a – f, a-0.15 (a-SiO <sub>2</sub> ), b-0.195 (borosilicate-bs), c-0.227 (soda-lime-silica: SLS), d-0.248 (SLS), e-0.264 (SLS), and f-0.298 (fluorite) g & h- bs at 1N, 98.1 N respectively. i) to l): SLS glass for 49 N load at 20, 200, 450 and 480 °C ( <i>Rouxel et al., 2021</i> )	13
Figure 2.6	Set of optical images obtained at varying normal load ( <i>Barlet et al., 2015</i> )	16
Figure 2.7	(a) Typical load vs displacement plots for ion exchanged aluminosilicate glasses (b) Zoomed view of the loading portion ( <i>Li et al., 2018</i> )	17
Figure 2.8	Schematic illustration of (a) indentation and (b) scratch ( <i>Prasad et al., 2009</i> )	19
Figure 2.9	Schematic illustration of the load-bearing area ( $A_{LB}$ ) due to scratching, cross-sectional projected scratch area ( $A_P$ ) which includes the pile-up consideration in the groove width measurement ( <i>Totten, 2017</i> )	22
Figure 2.10	(a) Schematic illustration of the lateral nanoindentation test using edge forward Berkovich geometry ( <i>de Macedo et al., 2018</i> ) (b) cono-spherical indenter tip (Front view indicates the projected tangential area) ( <i>Sawamura et al., 2019</i> )	24
Figure 2.11	Schematic representation of the scratch damage evolution in oxide glasses under monotonically increasing load (Scratch direction is from left to right) ( <i>Le Hou��rou et al., 2003</i> )	28
Figure 2.12	Representative AFM scan profile of the residual scratch groove ( <i>Moayedi et al., 2018</i> )	29
Figure 4.1	High temperature furnace along with the hot plate and steel mould used for preparing glasses using melt-quenching method	39
Figure 4.2	(a) Single-disc polishing unit (b) Low speed cutting machine	40

Figure 4.3	Vickers microhardness tester, Shimadzu HVM, 2 used in the Vickers residual indentation procedure	42
Figure 4.4	Vickers hardness tester machine used in the crack resistance measurements (Zwick Roell, model: ZHU/Z2.5)	44
Figure 4.5	ASMEC universal nanoindenter machine equipped with Nainite Nanosurf AFM workstation	45
Figure 4.6	Schematic representation of the vertical cross section of the nanoindentation at $P_{max}$	47
Figure 5.1	(a) Representative AFM image of the residual impression of 75B glass specimen investigated in this study (b) Schematic representation of the elastic reconstruction approach, where $h_f$ stands for final residual depth, and $h_c$ stands for elastically reconstructed contact depth from the final residual depth	54
Figure 5.2	Representative optical micrographs of residual imprint by Vickers indenter (a) 0B (b) 37B (c) 75B	56
Figure 5.3	Load-displacement curves acquired using nanoindentation technique of different glass samples used in this study	57
Figure 5.4	Representative Plots of (a) Hardness (b) Elastic modulus over depth of different glass samples used in this study by CSM procedure at 50 mN	58
Figure 5.5	(a) $1-h_c/h_{max}$ ratio, showing the elastic deformation, obtained from nanoindentation tests for different glass samples. (b) $1-h_f/h_{max}$ obtained from nanoindentation showing the elastic recovery of different glasses and their dependence on the hardness (Filled symbols are representing polished and unfilled for annealed glass samples)	60
Figure 5.6	(a) Representative AFM image of the residual impression of 75B glass specimen (Polished) investigated in this study (b) and its corresponding depth profile	62
Figure 5.7	Plot showing the relationship between the elastic reconstruction constant values and estimated hardness values of different glasses used in our study. (Filled symbols are representing polished and unfilled for annealed glass samples)	66
Figure 5.8	(a) $1-h_c/h_{max}$ ratio obtained from the depth profile obtained using AFM scan over the residual Berkovich impression of glasses used in our study. It is showing the AFM estimation of elastic deformation of the glasses and their dependence on hardness. (b) $1-h_f/h_{max}$ showing the AFM estimation of elastic recovery of the glasses and their dependence on hardness values. (Filled symbols are representing polished and unfilled for annealed glass samples).	67

Figure 5.9	(a) Relationship between $1-(h_c/h_{max})_{NI}$ (elastic deformation estimated by nanoindentation) and $1-(h_c/h_{max})_{AFM}$ (elastic deformation determined by AFM). (b) Relationship between $1-(h_f/h_{max})_{NI}$ (elastic recovery estimated by nanoindentation) and $1-(h_f/h_{max})_{AFM}$ (elastic recovery determined by AFM). (Filled symbols are representing polished and unfilled for annealed glass samples)	68
Figure 5.10	Plot showing the relationship between changes in hardness with final elastic recovery determined by AFM. (Open symbols indicate the annealed glass specimens and filled symbols indicate the polished specimen of the same composition)	69
Figure 6.1	(a) Typical AFM image of a residual Vickers impression (dotted line is drawn to reveal the corresponding depth profile for the impression), (b) Depth profile revealing the evolution of the impression before (red solid line) and after (black dotted line) annealing. $V_i^+$ , $V_i^-$ indicates the volume above and below the surface (blue dotted line) before annealing. Similarly, $V_a^+$ , $V_a^-$ represents the volume above and below the surface after annealing. $h_i$ and $h_a$ stand for depth below the surface before and after annealing, respectively. The depth profile corresponds to the 62B-12Si borosilicate glass specimen. (c), (e) Represents the typical 2D and 3D view of a residual Vickers impression before annealing, respectively. (d), (f) Represents the typical 2D and 3D view of residual Vickers impression after annealing, respectively	76
Figure 6.2	Load displacement curves of borosilicate glass samples of different compositions used in the present study	79
Figure 6.3	(a) $1-h_f/h_{max}$ ratio showing the elastic recovery obtained from nanoindentation tests for different borosilicate glass samples. (b) $1-h_c/h_{max}$ ratio obtained from nanoindentation showing the elastic deformation of different borosilicate glasses and their dependence on the hardness	81
Figure 6.4	Composition dependence of the maximum penetration depth ( $h_{max}$ )	82
Figure 6.5	Relation between the hardness and $[SiO_2]/([SiO_2] + [B_2O_3])$ molar ratio ( $K$ value). Comparisons are drawn between nanohardness and microhardness	84
Figure 6.6	Relation between hardness and network modifiers to boron molar ratio ( $R$ value)	86
Figure 6.7	Relation between the indentation pileup before annealing and the network modifiers to boron molar ratio ( $R$ value)	88
Figure 6.8	Relation between the fractional volume recovery ( $V_R$ ) estimated by following Yoshida et al. (Yoshida et al., 2005) protocol and the network modifiers to boron molar ratio ( $R$ value)	90

Figure 6.9	Relation between the fractional volume pileup ( $V_P$ ) and the network modifiers to boron molar ratio ( $R$ value)	92
Figure 6.10	Variation of the inverse of volume recovery ( $V_R$ ) with respect to hardness	93
Figure 7.1	Representative depth profile plots of (a) Hardness (b) Elastic modulus as a function of depth for different glass samples used in the present study by QCSM procedure at 50 mN	98
Figure 7.2	Load displacement (Ph) curve of sodium aluminophosphosilicate base glass with different ion-exchange timings	99
Figure 7.3	(a) Normal hardness measured from nanoindentation Ph Curve, (b) Indentation modulus measured from unloading portion of the Ph curve as a function of ion-exchange duration	100
Figure 7.4	(a) Scratch hardness values of sodium aluminophosphosilicate base glass ion exchanged at different timings (b) AFM image of the scratch track made using conospherical tip at 25mN normal load and the corresponding depth profile with red triangle markers indicating the measurement of scratch width in the scratch hardness estimation	102
Figure 7.5	(a), (b) $I-h_f/h_{max}$ ratio showing the elastic recovery obtained from nanoindentation under normal loading for base and ion-exchanged glass samples for different duration with respect to normal hardness and indentation modulus values. (c) $I-h_f/h_{max}$ ratio showing the elastic recovery under lateral loading with respect to scratch hardness values for sodium aluminophosphosilicate base glass, and ion-exchanged glass for different duration	104
Figure 7.6	Residual Vickers indentation images of sodium aluminophosphosilicate base glass and K-ion exchanged glasses at different applied normal loads	106
Figure 7.7	Residual Vickers Indentation image at 150 N of K30 specimen depicting its damage/crack resistance	107
Figure 7.8	SEM image of the scratch damage evolution in base glass (K-0) and ion-exchanged glass (K-15)	108

# List of Tables

		<b>Page No.</b>
Table 5.1	Composition (mol%) of the Glass Samples used in this study	52
Table 5.2	Glass hardness ( $H_v$ ) measured by the Vickers microindentation test at a load of 250 mN	57
Table 5.3	Analyzed hardness values and the corresponding maximum depth ( $h_{max}$ ), contact depth ( $h_c$ ), final depth ( $h_f$ ), $h_f/h_{max}$ , $h_c/h_{max}$ values for the investigated glass samples (0B, 37B, 75B) using nanoindentation	63
Table 5.4	Analyzed hardness values and the corresponding elastic reconstruction constant ( $e_c$ ), contact depth ( $h_c$ ) and recovered final depth ( $h_f$ ) post unloading, $h_f/h_{max}$ , $h_c/h_{max}$ values calculated using AFM for the investigated glass samples	64
Table 5.5	Calculated indentation hardness and contact hardness values by taking pile-up into consideration	65
Table 6.1	Experimental glass composition in mol % and other properties	73
Table 6.2	Indentation modulus values for the different borosilicate glass samples and the corresponding elastic recovery index ( $1-h_f/h_{max}$ ) and elastic deformation index ( $1-h_c/h_{max}$ ) values estimated using nanoindentation	80
Table 6.3	Experimental values of nominal mean diagonal length ( $d_i$ ), indentation depth ( $h_i$ ), volume below ( $V_i^-$ ) and above ( $V_i^+$ ), % indentation pile-up ( $V_i^+ / V_i^-$ ) obtained from AFM images of the various borosilicate glasses indented using Vickers geometry before annealing	87
Table 6.4	Experimental values of nominal mean diagonal length ( $d_a$ ), indentation depth ( $h_a$ ), volume below ( $V_a^-$ ) and above ( $V_a^+$ ), % volume recovery ( $V_r$ ), % volume pile-up ( $V_p$ ) obtained from AFM images of the various borosilicate glasses indented using Vickers geometry after annealing	89
Table 7.1	Maximum penetration depth ( $h_{max}$ ), final depth ( $h_f$ ), elastic recovery ratio ( $h_f/h_{max}$ ), indentation hardness and modulus values obtained using nanoindentation for sodium aluminophosphosilicate base and its ion-exchanged glasses	101